FRACTURE SIMULATION OF CONCRETE BY VISCO-ELASTO-PLASTIC SUSPENSION ELEMENT METHOD

T. HIRAIWA, Y. NANBU, M. ARAI, Y. KUROKAWA,
H. MORI and Y. TANIGAWA
Dept. of Architecture, Graduate School of Engineering, Nagoya Univ.,
Nagoya, JAPAN

Abstract

The authors have proposed visco-elasto-plastic suspension element method in order to simulate the fracture behavior of hardened concrete. In this analytical method, a simplified non-continuum model for aggregates and matrix is used, and the equation of motion is solved by the dynamic simulation method.

In this paper, the details of this analytical method and the analytical results are described.

Key words : Dynamic analysis, non-continuum model, visco-elasto-plastic suspension element method

1 Introduction

The deformation and fracture behavior of concrete have been already investigated in many experimental studies, and various constitutive models representing the stress-strain relation have been proposed based on these results. However, the mechanical properties of concrete have been explained only qualitatively because of complicated characteristics of concrete as a composite material.

Moreover, though most of experimental results have been obtained by small specimens under simple static loading condition, actual concrete structures become much larger in recent years, and most of failures of concrete in these structures occur under high-speed, repetitive and combined loads. Therefore, it is necessary to make the analytical model applicable to express the strength and fracture behavior of concrete theoretically.

In this paper, a new analytical method applicable to composite materials such as concrete is proposed, and some examples of analytical results are shown. Because of dynamic solution in this method with non-continuum model, the deformation and fracture behavior, including the occurrence and development of internal cracks, can be simulated dynamically.

2 Visco-elasto-plastic suspension element method

The visco-elasto-plastic suspension element method (VEPSEM) is developed by supplementing the elasticity and the failure criterion into viscoplastic suspension element method (VSEM) which had been proposed to simulate the flow behavior of fresh concrete.

2.1 Suspension element
Figure 1 shows the suspension element used in this analysis. In this analytical method, the simple non-continuum model with nodal point for aggregate and suspension element for matrix mortar between aggregates is used. The suspension element is consisted of elastic spring, viscous dashpot and plastic slider in axial and shear directions of the element. It is thought that most of cracks in hardened concrete happen in matrix mortar or in interfacial zone between matrix mortar and aggregate. Therefore, in this analysis, the deformation of aggregate is disregarded, and the shape of aggregate is assumed as sphere.

When the distance between two aggregates is shorter than the input value of limit distance, a cylindrical visco-elasto-plastic suspension
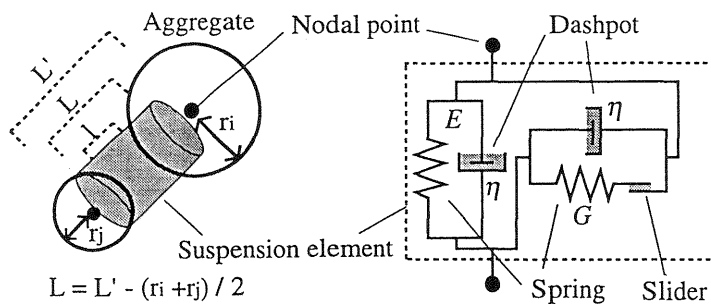

L = L' - (ri +rj) / 2

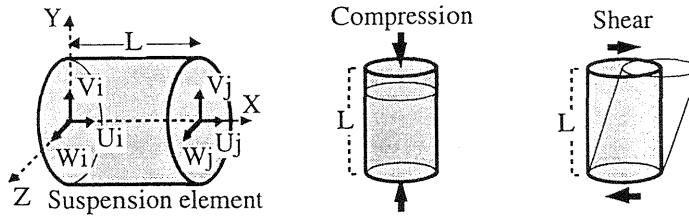Fig. 1. Suspension element and nodal point

Fig. 2. Coordinate and deformation of susupension element

element is constructed between these aggregates, and stress is transmitted by this suspension element. The radius of suspension element is the same as that of smaller aggregate. In this calculation, the limit distance is constant, though it is thought that this value needs to be changed by mix proportion. Fig. 2 shows the deformation of suspension element, axial and shear strains are calculated in this analysis, and the bending deformation of element are disregarded.

The boundary condition can be considered as loading boards. A vertical element for loading boards is constructed between dummy nodal point projected on loading board and nodal point. The loading in this analysis is expressed by moving of dummy nodal points on loading boards at constant loading rate.

2.2 Failure criterion

Figure 3 shows the constitutive law used in this analysis. The parameters of this constitutive law are yield value τ_y, plasticity η used in Bingham's model, and moduli of elasticity in axial and shear directions.

Figure 4 shows the failure criterion based Mohr-Coulomb and the rheological models in each stress in this analysis. Equation (1) is the failure criterion defined by pure tensile strength Ft and the angle of internal friction ϕ. The pure compressive failure is not considered.
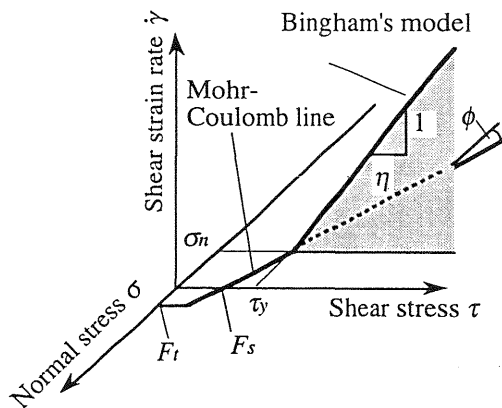

Fig. 3. Constitutive law

$$\tau > F_s - \sigma_n \cdot tan\phi \qquad \text{or} \qquad \sigma_n > F_t \qquad\qquad (1)$$

where, τ : shear stress, F_s : pure shear strength assumed $F_s = 2F_t$ in this analysis, σ_n : tensile axial stress, ϕ : angle of internal friction, F_t : pure tensile strength.

The yield value used in Bingham's model depends on axial stress and is defined in the next equation.

$$\tau_y = F_s - \sigma_n \cdot tan\phi \qquad\qquad (2)$$

where, τ_y : yield value.

The state of suspension element depends on stress condition in each element. The Each rheological model is explained as follows:

Phase 1 ; In this phase, the element is not in failure. A visco-elastic element is constructed in axial and shear directions. The element can't return to this phase after failure because it is an irreversible phenomenon.

Phase 2 ; In this phase, the element is in failure under axial compressive stress. A visco-elastic element is constructed in axial direction, and a visco-plastic element is constructed in shear direction.

Phase 3 ; In this phase, the element is in failure under axial tensile stress. The element is not constructed in both axial and shear directions.
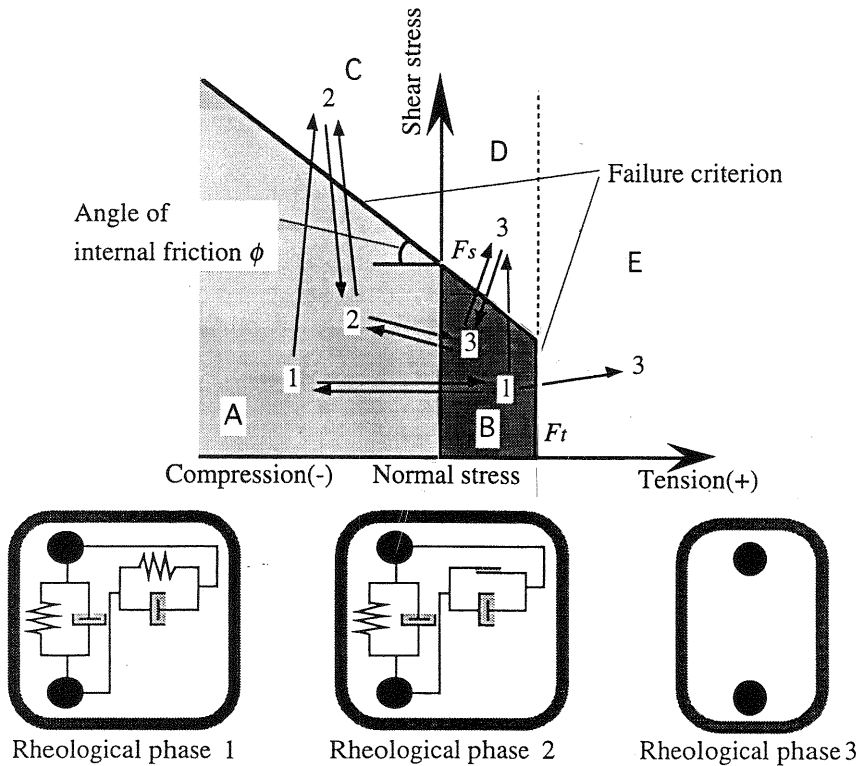

Fig. 4. Failure criterion and rheological models

942

2.3 Characteristics of this analytical method

VEPSEM is based on the equation of motion shown as the following two equations.

$$M\ddot{u} + C\dot{u} + K u - f = 0 \qquad (3)$$
$$I\ddot{\varphi} + C\dot{\varphi} + K \varphi = 0 \qquad (4)$$

where, M : mass matrix, C : visco-plastic matrix, K : elastic matrix, u : displacement vector, φ : angular displacement vector, I : moment of inertia, f : nodal force vector.

There are two characteristics in this analysis. First, the use of a simple non-continuum model consisted of aggregates and matrix makes the calculation simple. Secondly, the dynamic analysis can be carried out by solving the equation of motion. The advantage of the former is to be able to express the complex behavior of concrete by this simple model, and the advantage of the latter is to be able to consider the influence of intense change of velocity by occurrence of internal cracks. However, large calculation memory and time are demanded. Therefore, 2-dimensional model is used in this paper, though the analysis used 3-dimensional model is possible.

3 Analytical results

3.1 Compressive test

The simulations of compressive test by using this analytical method were carried out as uniaxial compressive test, biaxial compressive test and repetitive compressive test. However, only the result of uniaxial compressive test is discussed in the limited number of the following pages.

Figure 5 shows the analytical model for simulation of compressive test. The influences of pure tensile strength and angle of internal friction on the fracture behavior of concrete are investigated. The input data used in this analysis are shown in Table 1. The strain is calculated from the distance between loading boards, and the stress is obtained by the following equation.

$$\sigma_c = P / A \qquad (5)$$

where, σ_c : compressive stress (MPa), P : compressive load (N), A : section area (m^2).

Figure 6 shows the influence of pure tensile strength on the shape of stress-strain curve. The compressive strength of concrete and the strain at maximum stress increase with increasing in the pure tensile strength
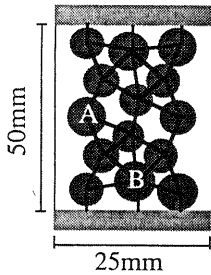
Fig. 5. Analytical 14B model

50mm

25mm

Table 1. Input data

Test	$\tan\phi$	F_t	E	η
Uniaxial compressive test	0.1, 0.2, 0.3	1, 2, 3	21	0.5

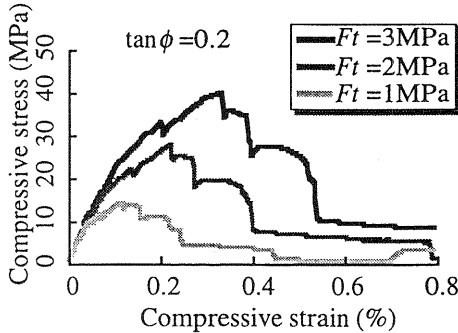[Notes] ϕ : Angle of internal friction, F_t : Pure tensile strength (MPa), E : Elastic modulus (GPa), η : Viscosity (MPa·s)

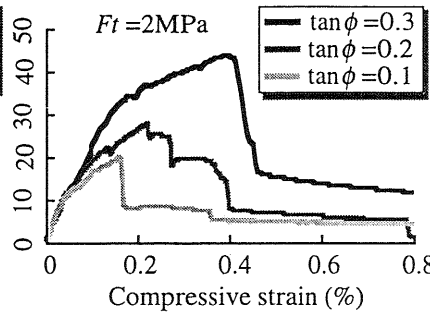Fig. 6. Influence of pure tensile strength on stress-strain curve

Fig. 7. Influence of internal friction strength on stress-strain curve

proportionally, though the elastic modulus is almost same independently of the pure tensile strength.

Figure 7 shows the influence of internal friction on the shape of stress-strain curve. According to this figure, the shape of stress-strain curve is changed and the compressive strength of concrete increases with increasing in the internal friction.

3.2 Tensile test

The simulations of tensile test by using this analytical method are applied to direct tensile test and tensile splitting test. However, only the result of tensile splitting test is discussed in the limited number of the following pages. The input data used in this analysis are shown in Table 2.

Figure 8 shows the analytical model used in the simulation of tensile splitting test. The lateral strain is calculated from the displacement between X and X' shown in Fig. 8. The tensile stress is obtained by the following equation.

$$\sigma_t = 2P / (\pi dL) \tag{6}$$

where, σ_t : tensile stress (MPa), P : load (N), d : diameter of cylindrical specimen (m), L : length of cylindrical specimen (m).
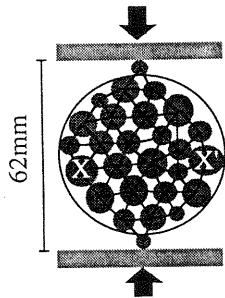
944

Fig. 8. Analytical
27B model

Table 2. Input data

Test	Model	$\tan\phi$	Ft	E	η
Tensile splitting test	14B model	0.1, 0.2, 0.3	1, 2, 3	21	0.5
Bending test	14Bb model 20Bb model	0.2	2		

[Notes] ϕ : Angle of internal friction, Ft : Pure
tensile strength (MPa), E : Elastic
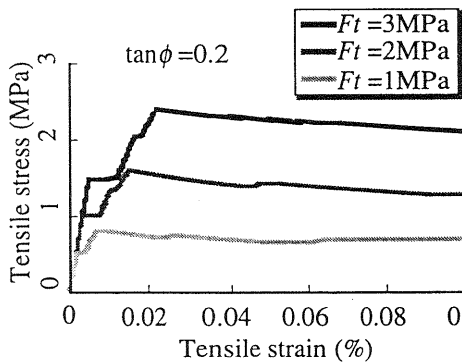modulus (GPa), η : Viscosity (MPa·s)

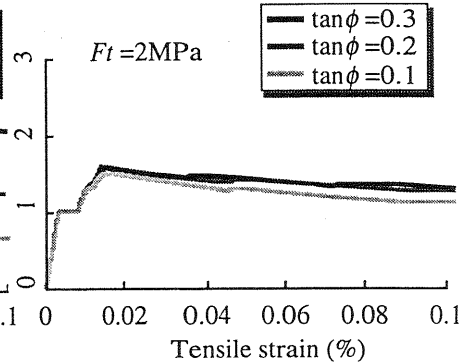Fig. 9. Influence of pure tensile
strength on stress-strain curve

Fig. 10. Influence of internal friction
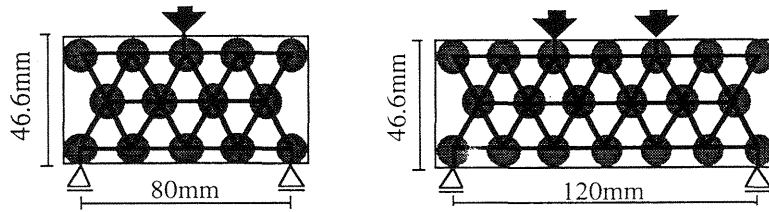strength on stress-strain curve

Figure 9 shows the influence of the pure tensile strength on tensile
stress-strain curve. Though the tensile strength of concrete is
proportional to the pure tensile strength, the former is a little smaller than
the latter.

Figure 10 shows the influence of the angle of internal friction on the
tensile stress-strain curve. The stress-strain curve is almost same
independently of the angle of internal friction. This tendency is different
from the simulational result of compressive test mentioned above.

3.3 Bending test

The bending failure tests of concrete beam by center-point loading and by
third-point loading are simulated by using two analytical models shown in
Fig. 11. The input data used in this analysis are shown in Table 2.

Figure 12 shows the influence of the pure tensile strength on the
bending deformational behavior of concrete by center-point loading
method and by third-point loading method. The bending stress is
obtained by the following equation.

(a) 14Bb model for center-point loading (b) 20Bb model for thrid-point loading
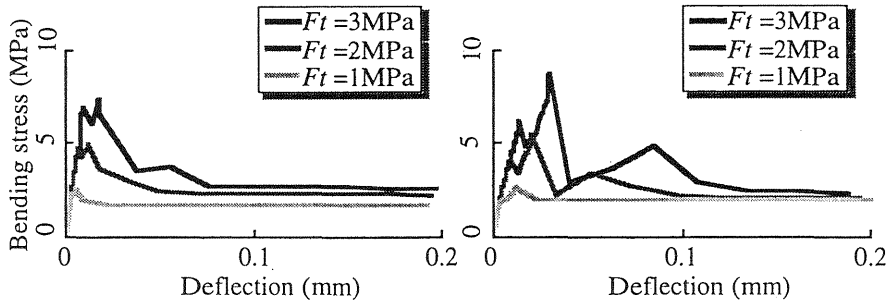
Fig. 11. Analytical models

Fig. 12. Influence of pure tensile strength on
relationship between bending stress and deflection of center

$$\sigma_b = M / Z \tag{7}$$

where, σ_b : bending stress (MPa), M : maximum bending moment (N·m), Z : section modulus (m³).

Comparing with these figures, the bending strength of concrete increases almost proportionally to the pure tensile strength in both loading methods, and the difference caused by the loading method is considered to be slight.
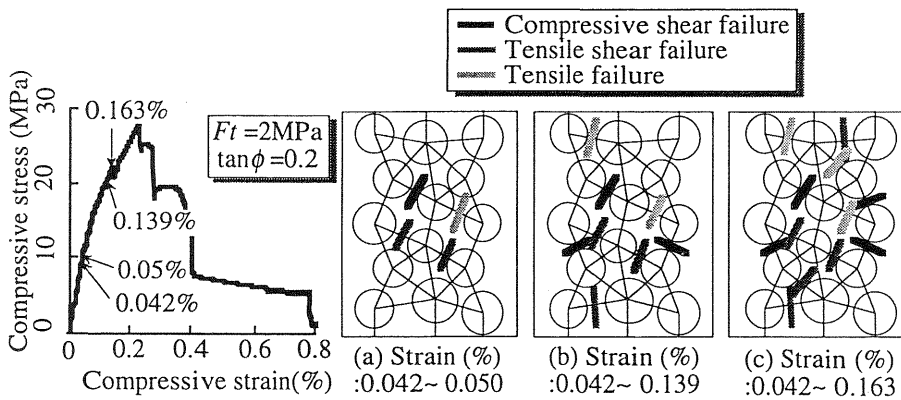

(a) Strain (%) :0.042~0.050
(b) Strain (%) :0.042~0.139
(c) Strain (%) :0.042~0.163

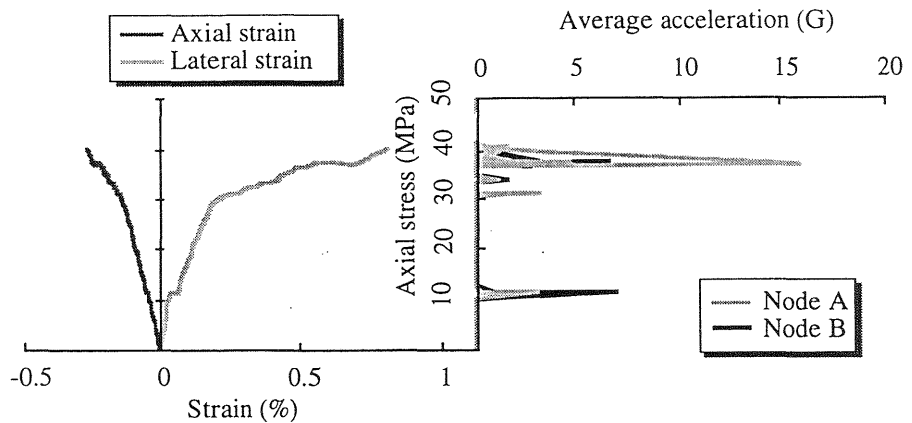Fig. 13. Progress of internal cracks

Fig. 14. Relationship between stress-strain-average acceleration

3.4 Progress of internal cracks

The progress of internal cracks is considered by the analytical result.   In this analysis, the stress is calculated for all elements at each time step, and the rheological model is selected according to the stress state. Compressive shear failure, tensile shear failure and pure tensile failure are considered.

Figure 13 shows a result of the progress of internal cracks. According to this figure, the internal cracks occur in the center portion of model by Poisson's effect after loading, and they progress to the outer portion.   Though the shear tensile failure and the pure tensile failure mostly occur in lateral directed elements, the compressive shear failure occurs independently of the direction of element.

3.5 Simulation of acoustic emission

Figure 14 shows the average acceleration in each incremental time at nodes A and B shown in Fig. 5 with the relationship between stress and strain.   The large acceleration is observed at each turning point on stress-strain curve, and the largest one is observed at maximum stress.   It is caused from that the failure occurs in many elements.

Comparing nodes A and B, the acceleration at node A is usually larger than that at node B.   It shows that the acoustic emissions mostly occur in the center portion of specimen, and progress to the outer side.

4 Conclusion

The purposes of this study are to investigate the mechanism of fracture and deformational behaviors of concrete as a composite material from a microscopic point of view, to explain theoretically the constitutive law of concrete, and to propose a more general model.

In this study, authors have proposed a new analytical method to simulate the fracture behavior of concrete, and shown the analytical results by using this method.

According to the results shown in this paper, it was confirmed that the fracture and deformational behaviors of concrete under various kinds of loading conditions can be analyzed by this method.

5 Acknowledgments

6 References

Arai M., Tanigawa Y., Mori H. and Kurokawa Y. (1995) Analytical study on tensile and bending failures of concrete by visco-elasto-plastic suspension element method. **Transactions of JCI**, 17, 85-92.

Arai M., Funami T., Kurokawa Y., Mori H. and Tanigawa Y. (1995) Failure analysis of concrete based on non-continuum model. **Transactions of AIJ**, 471, 1-9. (in Japanese)

Mori H., Watanabe K., Umemoto M. and Tanigawa Y. (1991) Flow analysis of fresh concrete as s two phase model. **Transactions of AIJ**, 427, 11-21. (in Japanese)

Mori H., Arai M., Funami T., and Tanigawa Y. (1993) Study on analytical method of concrete failure by suspension element method. **Transactions of JCI**, 15, 155-162.

Rossi, P. and Richer, S. (1987) Numerical modeling of concrete cracking based on a stochastic approach. **Materials and Structures**, 20, 19, 334-337.

Schlangen, E. and van Mier, J. G. M. (1992) Experimental and numerical analysis of micromechanisms of fracture of cement-based composites. **Cement and Concrete Composites**, 14, 2, 105-118.

Vervuurt, A., van Mier, J. G. M. and Schlangen, E. (1994) Analyses of anchor pull-out in composites. **Materials and Structures**, 27, 169, 251-259.

Wittman, F. H. (1993) **Numerical models in fracture mechanics of concrete**. BALKMA, Switzerland.

Xiao, C. Z., Lian, H. Z. and Liu, X. L. (1994) Analysis of microstructure of hardened cement paste by finite element method. **Cement and Concrete Research**, 24, 1, 1-7.